Applied Radiation and Isotopes 121 (2017) 6–11

Contents lists available at ScienceDirect

Applied Radiation and Isotopes

journal homepage: www.elsevier.com/locate/apradiso

Development of a nickel plated aluminum krypton-81m target system

F. Alrumayan[a,*], S.M. Okarvi[a], K. Nagatsu[b], S. Yanbawi[a], I. Aljammaz[a]

[a] King Faisal Specialist Hospital and Research Centre, Department of Cyclotron and Radiopharmaceuticals, Research Centre, Riyadh 11211, Saudi Arabia
[b] Department of Radiopharmaceuticals Development, National Institutes for Quantum and Radiological Sciences and Technology, 4-9-1 Anagawa, Inage-Ku, Chiba 263, Japan

ARTICLE INFO

Keywords:
^{81}Rb
^{81m}Kr
Gas target
Cyclotron

ABSTRACT

A fully automated system was developed to produce rubidium-81 (^{81}Rb), based on the ^{nat}Kr (p, n) ^{81}Rb reaction. The energy incident on the target was 26 MeV. Only 6 MeV was stopped inside the gas and the remainder was stopped by a specially designed flange. The target body was characterized by its conical shape and its inner walls were chemically plated with 100 ± 10 μm of nickel (Ni). Ni is advantageous as a fairly good conductor of heat whose surface can resist solutions. Additionally, the Ni plated target allowed potassium chloride to dissolve ^{81}Rb, with no further effect on the target body. The system produced ^{81}Rb with a production yield of approximately 4.5 mCi/μA h, which is close to the calculated expected yield of 5.3 mCi/μA h. The system is able to deliver reliable and reproducible radioactivity for patients and can be operated up to 1500 μA h before preventive maintenance is due. Key steps in designing the ^{81}Rb target for selected energy ranges are reported here.

1. Introduction

Krypton-81m (^{81m}Kr), an attractive short half-life radionuclide ($T_{½}$ = 13.1 s) with a convenient 190 keV of gamma rays in high abundance (67%), is regarded as a useful radiotracer in nuclear medicine, particularly for lung ventilation studies (Acerbi et al., 1981; Ruth et al., 1985; Hanser and Feurer, 1981). In normal practice, ^{81m}Kr is obtained from a parent nuclide, ^{81}Rb ($T_{½}$ = 4.5 h) assembled in an ^{81}Rb/^{81m}Kr generator system. Several methods of ^{81}Rb production are reported and summarized as follows:1) Bombardment with ^{3}He of ^{79}Br or ^{80}Kr up to 21 MeV (Homma et al., 1979;); 2) Bombardment with ^{4}He of Na ^{nat}Br, or Cu_2 $^{nat}Br_2$ up to 50 MeV (Fremlin and Stewart, 1978; Homma et al., 1979); 3) Bombardment with deuterons of enriched ^{80}Kr or ^{82}Kr up to 22 MeV (Gindler et al., 1976; Acerbi et al., 1981); 4) Bombardment with protons of enriched ^{82}Kr, ^{83}Kr, ^{84}Kr, or ^{nat}Kr up to 33 MeV (Steyn et al., 1991; Acerbi et al., 1981; Gindler, 1976; Uhlir and Helus, 1996).

Among these methods, a proton-induced reaction gives higher yields (Uhlir and Helus, 1996). An additional significant advantage of using ^{nat}Kr can be expected over other methods, as these require laborious preparation and processing, whereas the ^{nat}Kr gas handling procedure is simple and easy to perform.

The selection of a target body for ^{81}Rb production is very important. Several materials for fabricating the target body have been proposed and evaluated. Selecting a suitable target material is crucial not only to minimize the risk of target failure but also to reduce the exposure of personnel, especially during maintenance. Although aluminum (Al) is the target body most commonly used to produce ^{81}Rb (Waters, 1986; Meyer, 1989; Mulders, 1984), several draw backs of its use have been reported (Lambrecht and Sajjad, 1988), including: i) corrosion of the target window, ii) diminished recovery yield of ^{81}Rb with repeated usage, iii) elution of metallic impurities along with ^{81}Rb. In response to these disadvantages, another group has used stainless steel, suggesting that it resists elution, corrosion and rapid oxidation (Finn, 1982). Alternatively, (Lambrecht and Sajjad, 1988) have reported the superiority of using nickel (Ni) over aluminum and its ability to produce consistent and predictable yields.

Other factors essential to the reliability of production are the shape and depth of the target chamber. Chamber depth is a function of pressure and energy (Wojciechowski et al., 1988). As the beam penetrates the gas medium, it progressively loses kinetic energy, while its diameter gradually increases with increasing depth, mainly due to coulomb-force interaction between the incident particles and the nuclei of the medium (Tárkányi et al., 1997). Therefore, a conical target has been the choice of many laboratories and is also adopted in this study.

This paper reports our development of an automated gas target system for routine production of ^{81}Rb via the ^{nat}Kr(p,n)^{81}Rb reaction using an aluminum target chemically plated with nickel. Details are given of target design, evaluation of a practical yield for ^{81}Rb/^{81m}Kr and preparation of an ^{81}Rb/^{81m}Kr generator, and its quality control is discussed.

* Correspondence to: Cyclotron and Radiopharmaceuticals Department, King Faisal Specialist Hospital and Research Centre, P.O. Box 3354, Riyadh 11211, Saudi Arabia.
E-mail address: rumayan@kfshrc.edu.sa (F. Alrumayan).

http://dx.doi.org/10.1016/j.apradiso.2016.12.008
Received 19 March 2016; Received in revised form 5 December 2016; Accepted 6 December 2016
Available online 13 December 2016

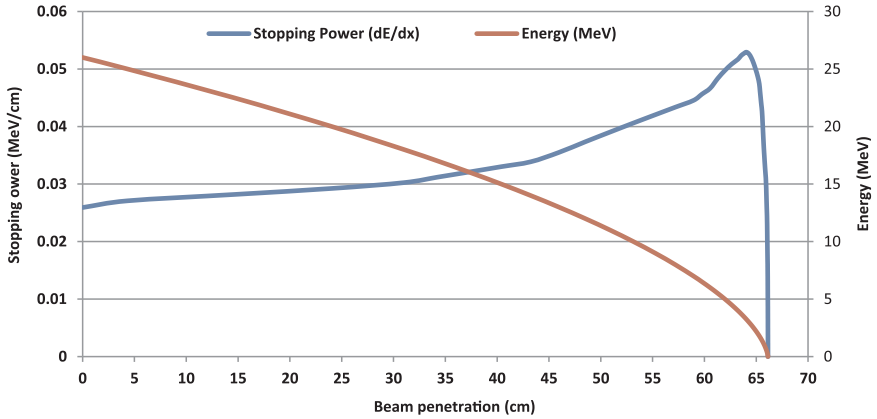

Fig. 1. Energy loss inside ^{nat}Kr. The blue curve shows stopping power with its Bragg peak (sharp peak) inside the ^{nat}Kr while the incident energy (red curve) continues degrading to minimal value, simulated with (SRIM, 2008). (For interpretation of the references to color in this figure legend, the reader is referred to the web version of this article.)

2. Materials and methods

Efficient production of ^{81}Rb leading to its daughter ^{81m}Kr requires determination of the energy of the particles inside the ^{nat}Kr target, taking into consideration the limitations of cyclotron energy. Target depth is a function of incident energy and gas pressure. Additionally, the incident proton beam is slowed down in ^{nat}Kr by the so called "stopping power" (dE/dx), where E is the particle energy (MeV) and x is the distance traveled (cm). The incident energy was decided to be 26 MeV (beam energy at the entrance). The stopping power was calculated with respect to a gas density of 0.0185 g/cm^3, which is equivalent to a pressure of 5.0 bar. Fig. 1 shows the stopping power of protons versus the kinetic energy of protons calculated from (SRIM, 2008). At that particular energy, the beam is stopped in a distance of 66.1 cm.

Unlike solid and liquid targets, where the material to be irradiated is confined in a small volume, gas targets are confined to a relatively large volume; and ^{nat}Kr, in particular, is not a very good heat conductor (Tárkányi et al., 1997). Therefore, it is more practical to eliminate the Bragg peak from being stopped inside the gas target to minimize heat developed inside.

The heat transfer inside gas targets generally involves a combination of both convection and conduction. It is assumed that three heat transfer process are involved during irradiations of gas targets; heat removal through the gas itself which involves a convective heat transfer, heat removal through the aluminum layer which involves conduction and heat removal through water channels which also involves convection.

The interaction pattern of protons at 26 MeV on ^{nat}Kr was simulated. The longitudinal trajectory of the beam is shown in Fig. 2. Layer 1 represents ^{nat}Kr with a density equivalent to 5 bar, layer 2 represents the solid aluminum plate at the back of the target, with density equivalent to 2.7 g/cm^3 and layer 3 represents water of density 0.9150 g/cm^3. Energies between 20 and 3.5 MeV are stopped in the entrance of the aluminum back plate. Protons below 3.5 MeV are stopped in water, including their Bragg peaks. Moreover, the beam typically spreads in gas targets due to multiple scattering, as shown in the simulation. To cope with this phenomenon and to avoid the beam striking the inner wall, the target body is usually designed to be conical. Additionally, the simulation clearly supports the idea of using beam stopper at the back of the target, where energy and Bragg peak can be completely absorbed.

Fig. 3 shows a cross-section of the conical target which was fabricated in house (front ∅ = 2.0 cm, back ∅ = 4.0 cm and target depth is 24.0 cm). The target volume is approximately 176 mL. At the front, the target is connected to a water-cooled aluminum collimator. The beam is collimated to an area of approximately 1.0 cm^2 before entering the target. A helium-cooled flange is placed between the

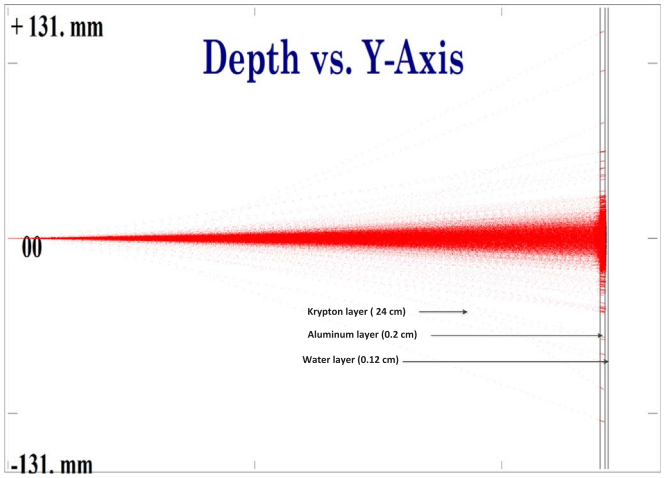

Fig. 2. Simulated two-dimensional projection of protons on krypton (longitudinal view), simulated with (SRIM, 2008). The distribution of particles (due to interaction with gas) has formed an angle of approximately 6° inside the target to which it was considered in the design of the target body.

collimator and the target. Attached to it, are two molybdenum foils; each is 40 μm (purchased from Goodfellow). Each foil absorb approximately 0.5 MeV of the incident energy. Helium is allowed to pass between at a flow rate of 1700 mL/min for cooling. Beam leaves the target at approximately 20 MeV, then passes through a special design flange, made of aluminum, where the beam is partially stopped at its entrance (Aluminum of 0.2 ± 0.02 cm), and the remaining energy is deposited in circulating water (0.12 ± 0.02 cm). The flange is composed of two parts attached to each other as shown schematically in Fig. 3a. The purpose of the flange is to absorb the rest of the energy. Its internal surface is designed in the form of fins to improve heat dissipation. The design is intended to promote an even distribution of the water at the back plate as shown in Fig. 3b.

It is important to note that if the beam is stopped in the circulating water, radioactive ammonia (^{13}N species) will be formed, due to the interaction of the beam with water (^{16}O(p,α)^{13}N). Therefore, the water circulation bath of this target is located inside the cyclotron vault so that personnel are not exposed to high-energy radiation.

The target body is electrically isolated from other parts to allow accurate beam current readings, which indicate the activity production rate inside the target. The flow rate and water temperature are 3.0 ± 0.3 L/min and 18 ± 1 °C respectively. The water temperature is of such a value as to eliminate water condensation on critical cyclotron components.

It is worth mentioning that the target was sent to an external company for chemical nickel–plating. Some specifications includes:

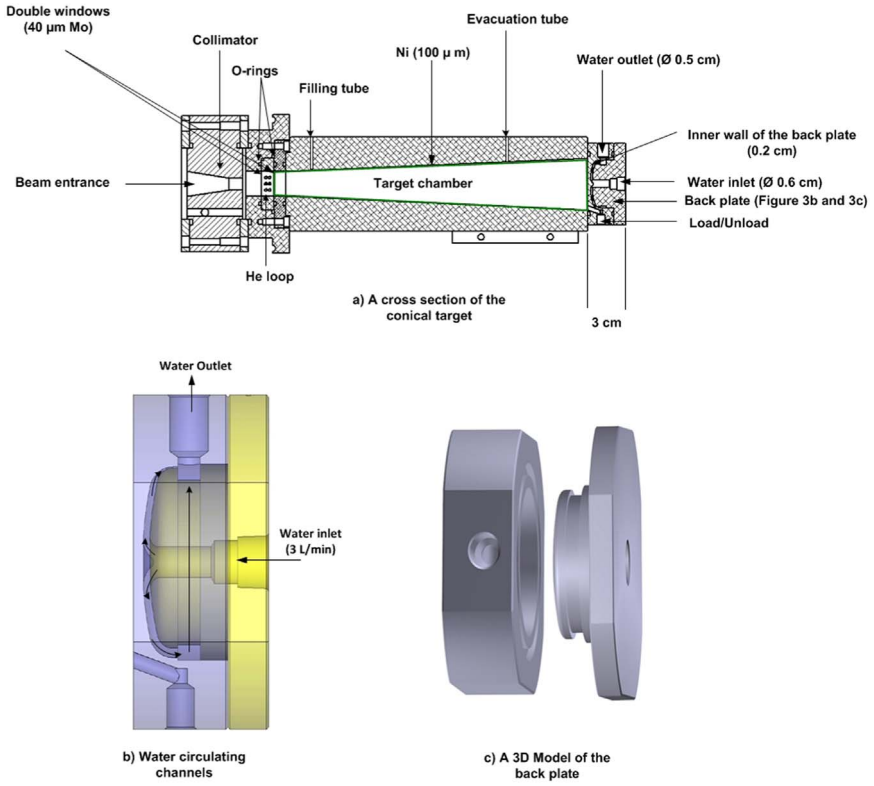

Fig. 3. Schematic diagram of the target chamber for the production of ^{81}Rb. Water circulating channels are shown in (b) and 3D model of the back plate is presented in (c).

purity of Ni is 99.99%, Ni-layer is completely uniform, smooth, homogeneous and strongly adherent. Thickness is 100 μm ± 10 μm. It is a non magnetic, glass-like and corrosion resistant surface.

The newly developed target system is shown in Fig. 4. The target was attached to port 4 in the cyclotron vault. Full access to the target loading/unloading steps was made through touch screen technology for user access. The FX3U Programmable Logic Controller (PLC) contributed to controlling the loading process, delivering the target solution and later, rinsing the target. Two algorithms were written to control the actions between the PLC and the external component on one hand, and the operator commands and the PLC on the other. Additionally, the target control system was designed to be protected by a chain of interlocked steps. The touch screen was developed so that the color of components would change to indicate an action taking place.

3. Experimental

The automated production cycle of ^{81}Rb is described below and a schematic representation of the system is given in Fig. 5. The target chamber was evacuated to approximately 10^{-3} mbar, then filled with ^{nat}Kr (Matheson TRI, Gas) at a pressure of 5 ± 0.5 bar. After irradiation, the ^{nat}Kr was cryogenically recovered and transferred to the original gas cylinder with losses of only approximately 0.3% during irradiation (calculated from the pressure of remaining gas at constant temperature). For full evacuation, all lines were evacuated to 10^{-2} mbar and the storage vessel (cold finger) was cooled to −140 ± 10 °C using liquid nitrogen. Consequently, the target pressure dropped to a low value indicating that the target was free of gas. The recovery process took about 5 min.

During irradiation with protons on ^{nat}Kr, ^{81}Rb was formed and deposited on the inner wall of the target body. The radioactivity produced in the target was removed by washing the target repeatedly with 0.001 mol/L of KCl and pumping it into hotcells using nitrogen gas (N_2), for chemical processing. An HPLC pump (Scientific System Inc., USA) was used to pump KCl into the target chamber at a flow rate

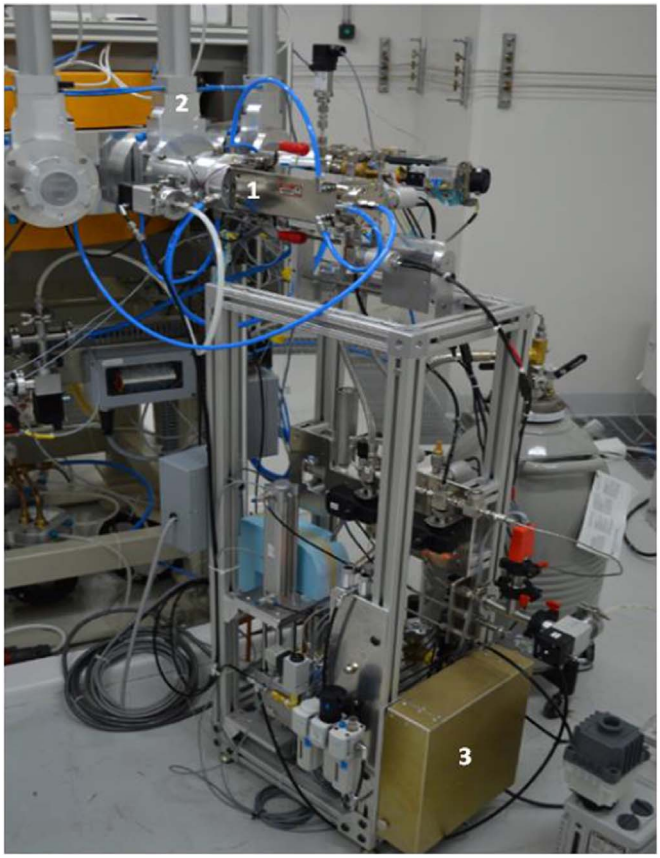

Fig. 4. Krypton target attached to the cyclotron beamline. Description of the target component is as follow: 1) target body, 2) cyclotron beam valve and 3) current reading circuitry.

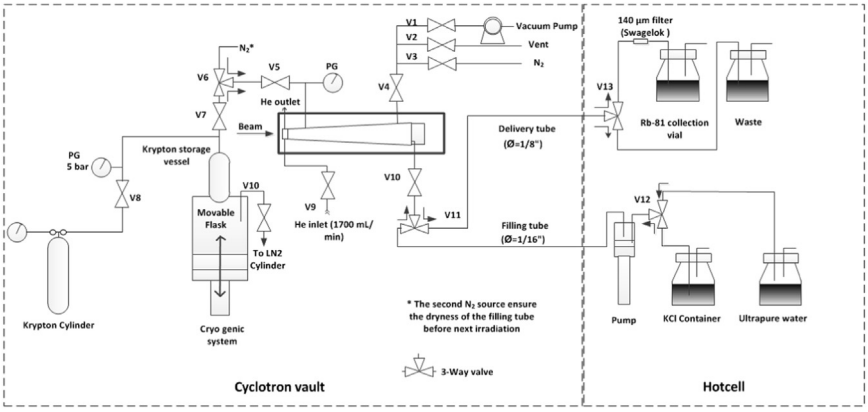

Fig. 5. Schematic diagram of the remotely controlled ^{81}Rb production system. The internal diameter of the delivery tube is chosen to be 1.5 mm to prevent it from being blocked by tiny particles from the target.

20 mL/min. After the removal of radioactive ^{81}Rb, the target was thoroughly rinsed using ultrapure water and dried with nitrogen and air for the next production cycle. The total activity obtained from first elution was above 90% and the remaining was collected from the second elution.

Expected yield of ^{81}Rb can be calculated from Eq. (1),

$$R = nI(1 - e^{(-\lambda t)}) \int_{Ef}^{E0} \frac{\sigma(E)}{(\frac{dE}{dx})} dE \quad (1)$$

where R is the number of nuclei formed per second; n is the target thickness in nuclei per cm^2; I is the incident particle flux per second, related to the beam current; λ is the decay constant; t is the irradiation time in seconds; σ is the reaction cross-section, or probability of interaction, expressed in cm^2, and is a function of energy; E (MeV) is the energy of the incident particles; x is the distance traveled by the particle in cm; and $\int_{Ef}^{E0}$ is the integral from the initial to final energy of the incident particle along its path. Fig. 6 represents the nuclear cross-section of the natKr(p, x)81Rb reaction. In order to calculate the expected yield for a selected energy range, σ was extrapolated from data in Fig. 6 (Acerbi et al., 1981; Kovacs et al., 1991; Steyn et al., 1991) and inserted into Eq. (1). The expected yield calculated for this target was 5.3 ± 0.5 mCi/µA h.

4. Results and discussion

4.1. Yield

The irradiations were performed in the C-30 cyclotron (from IBA) at King Faisal Specialist Hospital and Research Centre (KFSHRC). Several irradiations were performed with beam current and irradiation period of 15 µA and 30 min respectively. The average ^{81}Rb yield from the developed target was 4.5 ± 0.5 mCi/µA h (n = 3). A slight decrease in yield (about 85% of the expected value) could be explained partly by a density reduction of the target gas, particularly on the trajectory of proton beam. This consideration was not reflected in our calculation in Eq. (1).

During irradiation, interaction of the beam with ^{nat}Kr causes energy to dissipate in the form of heat. As a result, pressure increases inside the chamber. The entrance foils of the chamber must be thick enough to withstand the pressure differential, yet thin enough to absorb relatively little of the energy of the beam so that their temperature is maintained at a safe level. It is also important to determine the chamber temperature. However, it was not possible to measure the temperature inside the chamber directly; instead, an experiment was conducted to examine the safety of the target system and the durability of its foils with respect to the pressure level at the operating beam currents. Fig. 7 illustrates the behavior of the pressure as a function of beam current. Elevation in target temperature can be estimated from the increase in pressure during bombardment by applying the ideal gas law at constant volume and with the aid of Eq. (2) (Wojciechowski et al., 1988).

$$\Delta T = T_0\left(\frac{P}{P0} - 1\right) \quad (2)$$

The initial gas temperature is assumed to be 18 ± 1 °C (cooling water temperature). In this case, ΔT is 14.4 ± 1 °C.

In many cases, discontinuities in the heat transfer arise at the interfaces where two materials meet. Using the plating method, such as

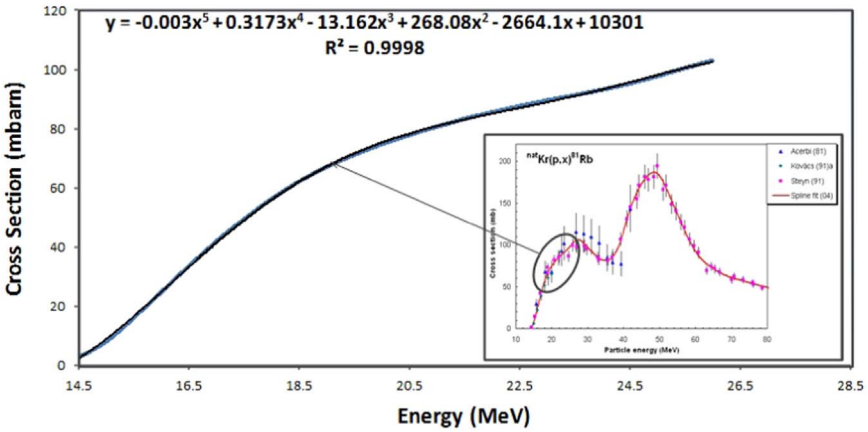

Fig. 6. Excitation functions for the formation of ^{81}Rb between 20 and 26 MeV. The curve describes a polynomial function fit to the experimental data obtained from the curve to the right (Acerbi et al., 1981; Kovacs et al., 1991; Steyn et al., 1991).

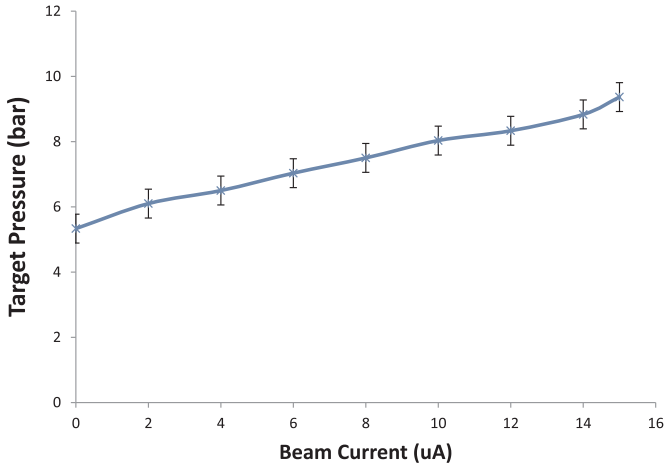

Fig. 7. Pressure in Kr gas as a function of beam current. The graph indicates safe operating pressure up to 15 uA (n = 3).

the Ni-plating used here, ensures better heat removal and makes it unlikely that target material will be lost or the target damaged during irradiation.

Under these conditions, it is safe to bombard the target and produce activity. It can be reliably operated up to 1500 μA h before foils are blown out. A visual inspection of the front foil (target side) has reveal a hot spot and a tiny hole in the middle. This is could be caused by the beam being too sharply focused. In other target systems, where helium cooling is not operated, front foil is rapidly blown out due to lack of heat removal.

4.2. Quality control characterization

The ^{81}Rb solution transferred to hotcell was tested before passing through the column generator to trap ^{81}Rb. The identifications of ^{81}Rb and other radionuclides were conducted using a HPGe detector coupled to a multichannel analyzer (DSA 1000, Canberra). The gamma spectra obtained were analyzed using Genie software (from Canberra, USA) and the results are presented in Fig. 8. As indicated in the graph, in addition to, ^{81m}Rb (81.1%), ^{81}Rb (10.1%), some impurities were also observed in the sample including ^{79}Rb (4.4%), ^{82m}Rb (4.2%), ^{83}Rb (0.1%) and ^{84}Rb (0.1%). At 12:00 noon (calibration time = 3 h after EOB), most of ^{81m}Rb ($T_{1/2}$ = 30 min), has decayed to ^{81}Rb, which in turns decays to ^{81m}Kr.

It is inherent to the production of ^{81}Rb via ^{nat}Kr that other concurrent isotopes are produced, but these do not interfere with the usefulness of ^{81}Rb.

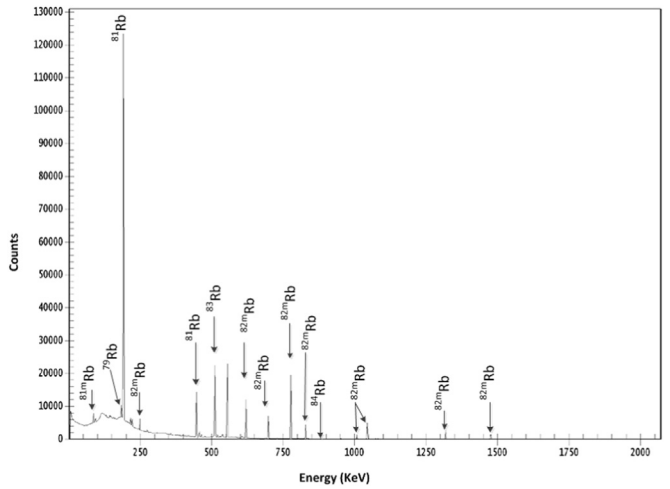

Fig. 8. Gamma-ray spectra of ^{81}Rb solution measured at EOB (Counting time is 60 min).

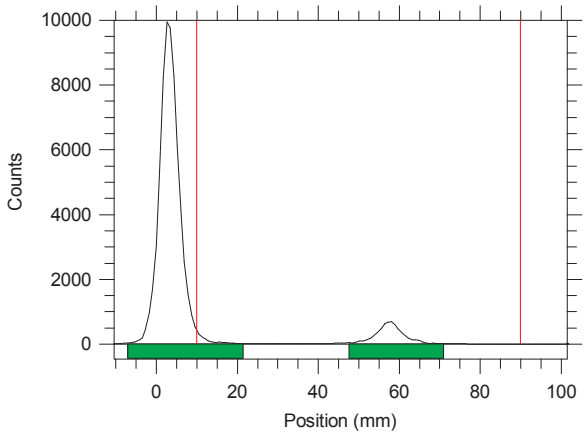

Fig. 9. Determination of the radiochemical purity of ^{81}Rb by TLC-SG using Acetone as the mobile phase. The main Peak near the origin represents the free rubidium ions.

4.3. Radiochemical purity of ^{81}Rb

Radio thin-layer chromatography (TLC) was performed on ^{81}Rb sample of 0.2 μCi. The sample (1 μL) was applied on TLC-SG sheet (2 × 10 cm), and using acetone as the mobile phase. After the run, scanning of the TLC strip was performed using AR-2000 radio-TLC Imaging Scanner (Bioscan, USA) and analyzed by WinScan software. The sample was measured at 3 h after the EOB and the chromatogram is shown in Fig. 9. The sheet was then cut into two pieces (origin and solvent front region) and the identification of the peaks was performed using gamma spectroscopy. The radiochemical purity of ^{81}Rb was found to be 91.0 ± 0.2% (n = 3). It is worth mentioning here that the sample mixture may contain some other Rb ions, such as ^{82m}Rb.

4.4. The generator

An Alltech SCX Maxi cartridge was used for preparing ^{81}R/^{81m}Kr generator. The efficiency of the column was 99.0 ± 0.5% (n = 3). A gas sample was obtained from the generator and was tested (3 h after the EOB) using gamma spectroscopy, in which the radionuclidic purity of ^{81m}Kr appeared to be 99.59 ± 0.1%. The spectrum is presented in Fig. 10. Other krypton daughters are produced during bombardment and represent a small fraction of the total activity (^{79m}Kr and ^{79}Kr were also observed at respective percentages of 0.34 ± 0.02% and 0.07 ± 0.01%). It is important to mention that these impurities were also detected from the ^{nat}Kr trapped after irradiation.

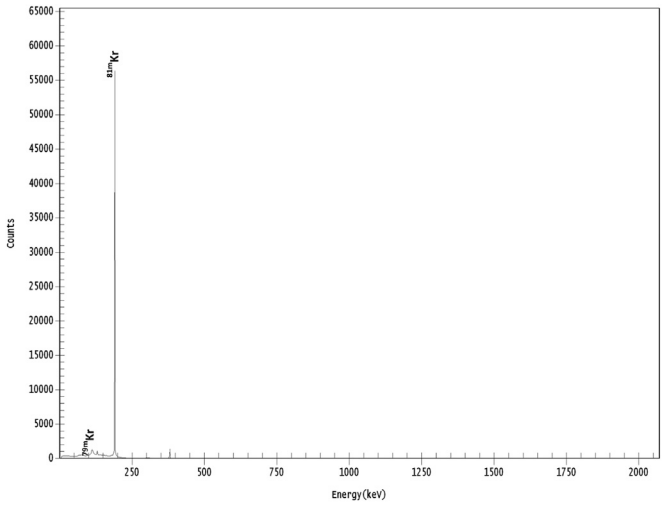

Fig. 10. Gamma-rays spectrum obtained from ^{81m}Kr gas sample (measured 3 h after the EOB).

At our hospital, each generator prepared for patients has an activity of 5–15 mCi of ^{81}Rb fixed on cation exchange resin. The effectiveness of personal radiation shields of the generator was calculated with respect to the lead shield used. The column generator is placed inside a cylindrical-shaped lead-shield (radius of the lead is 3.5 cm). At the calibration, each additional isotope in the generator (including its own gamma rays and their respective energies), is added to the overall dose. It was found that the external added radiation from the useful ^{81}Rb and other contaminants was 2 μSv/h at 1.0 m distance from the source. Thus, the shielding used for the generator at our hospital is adequate to minimize the external dose rate to an acceptable level.

5. Conclusion

The development of a reliable ^{81}Rb production setup based on ^{nat}Kr (p, x)^{81}Rb was presented in this paper. The existing approach provides full information on a systematic methodology for designing an ^{81m}Kr target system.

It is concluded that using a Ni-based plated target chamber made of aluminum permits a dilute KCl solution to dissolve ^{81}Rb deposited on the inner walls of the target chamber with the assurance of delivering a high yield, of approximately 4.5 mCi/μA h, as well as reliable production up to 1500 μA h of continuous operation. With such a long operating period, workers will not be exposed to high radiation due to repeated maintenance over a period of months. Additionally, ^{81m}Kr was tested on patients for ventilation imaging. It is safe to use in a clinical setting.

Acknowledgments

The Authors are grateful to Mr. John Schnider, Mr. Qassim Akkam and Sonny Wahab for excellent technical support. The Author would also like to thank Prof. Alsanea and Dr. Alsuhaibani (from King Saud University) for their contribution to useful discussions in heat transfer process. This project was jointly supported by KFSHRC and the NSTIP strategic technologies program in the kingdom. – Award No. (14-MAT-1233-20).

References

Acerbi, E., Bonardi, M., De Martinis, C., Salomone, A., 1981. Kr(p,xn) excitation functions and ^{81}Rb(^{81m}Kr) generator studies. Appl. Radiat. Isot. 32, 465–475.

Finn, R., Vora, M., Boothe, T., Campbell, J., Carroll, S., Clark, J., 1982. Radiation-induced defects as illustrated by the ^{81}Rb-^{81m}Kr target system. Int. J. Appl. Radiat. Isot. 33, 349–353.

Fremlin, S., Stewart, J., 1978. A new generator for krypton-81m. Nucl. Instr. Methods 156, 369–373.

Gindler, J., Oselka, M., Friedman, A., Mayron, L., Kaplan, E., 1976. A gas target assembly for the production of high purity, high specific activity ^{81}Rb. Int. J. Appl. Radiat. Isot. 27, 330–332.

Hanser, A., Feurer, B., 1981. Pure ^{81}Rb for medical use obtained by electromagnetic isotope separation. Appl. Radiat. Isot. 32, 775–778.

Homma, Y., 1979. Excitation functions for the production of ^{81}Rb(^{81m}Kr) via the ^{79}Br(α,2n)^{81}Rb and the ^{81}Br(3He,2n)^{81}Rb reaction. Appl. Radiat. Isot. 30, 345–348.

Kovacs, Z., Tarkanyi, F., Qaim, S., Stocklin, G., 1991. Excitation functions for the formation of some radioisotopes of rubidium in proton induced nuclear reactions of ^{nat}Kr, ^{82}Kr and ^{83}Kr with special reference to the production of ^{81}Rb(^{81m}Kr)generator radionuclide. Int. J. Appl. Radiat. Isot. 42, 329–335.

Lambrecht, R., Sajjad, M., 1988. Aluminum and nickel targets for rubidium-81 production. Int. J. Rad. Appl. Instr. Part A 39, 1081–1083.

Meyer, W., Plascjak, P., Finn, R., Sheh, Y., Regdos, S., Mignerey, A., 1989. A novel krypton gas target. Nucl. Instr. Methods Phys. Res. Sect. B 43, 112–115.

Mulders, J., 1984. Yield curves and beam current dependent production rates of Rb radioisotopes produced by protons on a krypton gas target. Int. J. Appl. Radiat. Isot. 35, 475–480.

Ruth, T., Adam, M., Burgerjon, J., Lenz, J., Pate, B., 1985. A gas target for radionuclide production with 500 MeV protons. Appl. Radiat. Isot. 36, 931–933.

Steyn, G., Mills, S., Nortier, F., Haasbroek, F., 1991. Integral excitation functions for ^{nat}Kr + p up to 116 MeV and optimization of the production of ^{81}Rb for ^{81m}Kr generators. Int. J. Rad. Appl. Instr. Part A 42, 361–370.

Stopping and Range of Ions in Matter, 2008. ⟨http://www.srim.org⟩.

Tárkányi, F., Takács, S., Heselius, S., Solin, O., Bergman, J., 1997. Static and dynamic effects in gas Targets used for medical isotope production. Nucl. Instr. Methods Phys. Res. Sect. A 21, 119–124.

Uhlir, G., Helus, F., 1996. A new ^{81}Rb-^{81m}Kr generator from enriched ^{82}Kr gas for medical use. J. Radioanal. Nucl. Chem. 204, 423–427.

Waters, S., Clark, J., Horlock, P., Brown, C., Bett, R., Sims, H., 1986. Production of ^{81}Rb using a 60 MeV proton beam Target development and aspects of recovery. J. Label. Comp. Radiopharm. 23, 1338–1340.

Wojciechowski, P., Sajjad, M., Lambrecht, R.M., 1988. A semi-quantitative approach to the design, analysis and operation of a gas target system. Appl. Radiat. Isot. 39, 429–436.